Preparation of Hyperbranched Structures of α-Fe_2O_3

Young-Sik Cho and Young-Duk Huh*

Department of Chemistry, Center for Photofunctional Energy Materials, Dankook University, Gyeonggi 448-701, Korea
**E-mail: ydhuh@dankook.ac.kr*
Received March 19, 2009, Accepted May 6, 2009

Key Words: Hyperbranched microstructure, Snowflake-like morphology, α-Fe_2O_3

Hierarchical structures of metal oxides comprised of nanoparticles, nanorods, and nanobelts as building blocks have attracted great interest due to their novel structures, properties, and applications.[1-3] However, the preparation of high-quality crystals with hyperbranched structures is a challenging issue. The majority of these structures are formed by hierarchical self-assembly mechanisms, and the snowflake-like morphology is a typical example of a hyperbranched structure. Considerable effort has been devoted to the synthesis of metal oxides and metal sulfides with snowflake-like morphologies.[4-7]

α-Fe_2O_3 is an n-type semiconductor with a band gap of 2.1eV, and is used today in catalysis, sensors, magnetic recording media, rechargeable lithium batteries, and as a pigment.[8-12] Various techniques have been used to synthesize α-Fe_2O_3 with rod, wire, spindle, flower, and dendritic morphologies.[13-16] However, relatively little is known of fabricating α-Fe_2O_3 with a snowflake-like morphology, and all successful attempts to date have involved the hydrothermal decomposition of $K_3[Fe(CN)_6]$, which makes it difficult to examine the evolution of hyperbranched structures due to the difficulty of controlling the decomposition rate of $K_3[Fe(CN)_6]$.[17-19] Here we report a simple method for producing hyperbranched structures of α-Fe_2O_3 based on a hydrothermal reaction in aqueous solutions containing KCN and $FeCl_3$.

Experimental Section

$FeCl_3 \cdot 6H_2O$ (Aldrich) and KCN (Aldrich) were used as received. In a typical procedure, a mixed solution containing 40 mL of 0.05 M $FeCl_3 \cdot 6H_2O$ and 40 mL of 2.00 M KCN was placed in a Teflon-sealed autoclave at 140 °C for 16 h. In order to investigate the evolution of the morphologies of the α-Fe_2O_3 crystals produced, different KCN concentrations (0.25 M, 0.50 M, 1.00 M, and 2.00 M) were used at fixed 0.05 M $FeCl_3$. To investigate the effects of concentration of $FeCl_3$, different $FeCl_3$ concentrations (0.001 M, 0.005 M, 0.01 M, and 0.05 M) were also used at fixed 1.50 M KCN. The products were filtered and washed with ethanol several times, and then dried at 60 °C for 12 h in an oven.

α-Fe_2O_3 crystal structures were analyzed by powder X-ray diffraction (XRD, Rigaku DMAX-ⅢA) using Cu Kα radiation, and crystal morphologies were characterized by scanning electron microscopy (SEM, Hitachi S-4300). The Raman spectra of the products were obtained with a Raman spectrometer (HORIABA Jobin Yvon T64000) using radiation of 514.5 nm from an argon ion laser.

Results and Discussion

Figure 1 shows the XRD patterns and Miller indices of the α-Fe_2O_3 crystals obtained from an aqueous mixture containing 40 mL of 0.05 M $FeCl_3 \cdot 6H_2O$ and 40 mL of 2.00 M KCN reacted at 140 °C for 16 h. Most of peaks were assigned to the rhombohedral phase of α-Fe_2O_3 and concurred with literature data (JCPDS 33-0664, a = 5.035 Å, c = 13.740 Å). The peaks asterisked around at 14° and 22° are unidentified. There are many iron oxides and iron oxyhydroxides such as hematite (α-Fe_2O_3), magnetite (Fe_3O_4), wüstite (FeO), goethite (α-FeOOH), lepidocrocite (γ-FeOOH). Since iron oxides and iron oxyhydroxides have their unique Raman spectra, Raman spectroscopy is a good method to examine iron oxides and iron oxyhydroxides. Figure 2 shows the Raman spectrum of the as-prepared product obtained from an aqueous mixture containing 40 mL of 0.05 M $FeCl_3 \cdot 6H_2O$ and 40 mL of 2.00 M KCN. All of Raman peaks correspond to those of α-Fe_2O_3. In the Raman spectrum of α-Fe_2O_3, the peak at 225 and 498 cm^{-1} were assigned to A_{1g} modes. The peaks at 247, 293, 412, and 613 cm^{-1} were also assigned to E_g modes. The intense peak at 1320 cm^{-1} is assigned to a two-magnon scattering which arise from the interaction of two magnons created on antiparallel close spin sites.[20] No other peaks were detected, indicating that this simple method yields only α-Fe_2O_3 free from other iron oxides and iron oxyhydroxides.

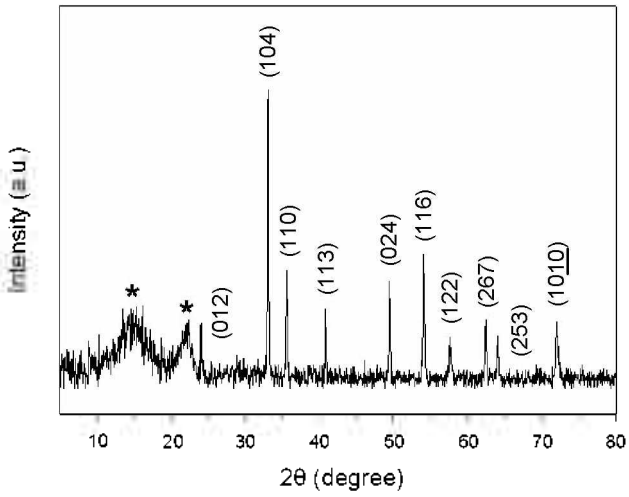

Figure 1. XRD pattern of snowflake-like α-Fe_2O_3 synthesized at [$FeCl_3$] = 0.05 M and [KCN] = 2.00 M under hydrothermal conditions for 16 h at 140 °C.

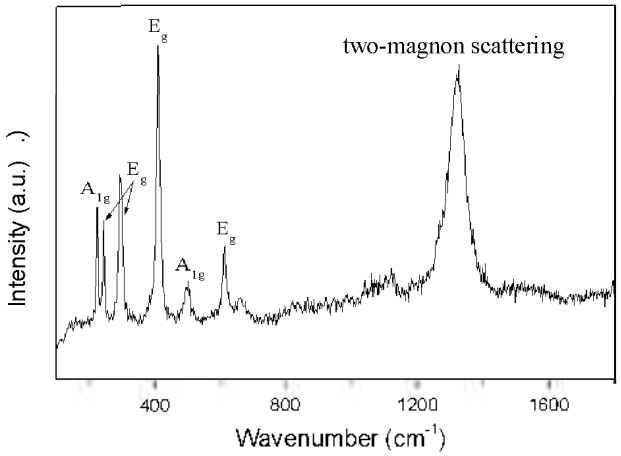

Figure 2. Raman spectrum of snowflake-like α-Fe_2O_3 synthesized at [$FeCl_3$] = 0.05 M and [KCN] = 2.00 M under hydrothermal conditions for 16 h at 140 °C.

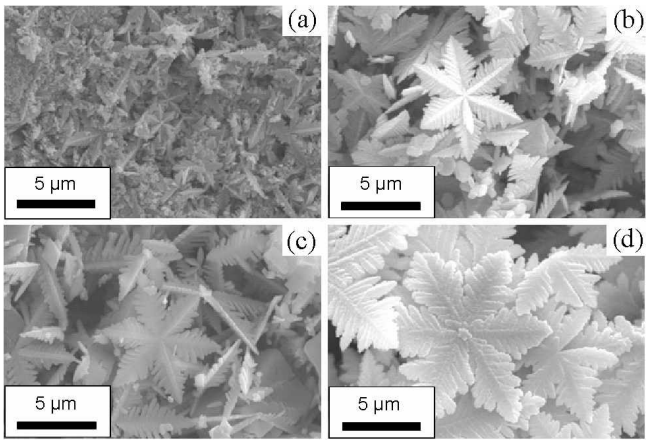

Figure 3. SEM images of α-Fe_2O_3 products obtained at [$FeCl_3$] = 0.05 M using different concentrations of KCN: (a) 0.25 M, (b) 0.50 M, (c) 1.00 M, and (d) 2.00 M.

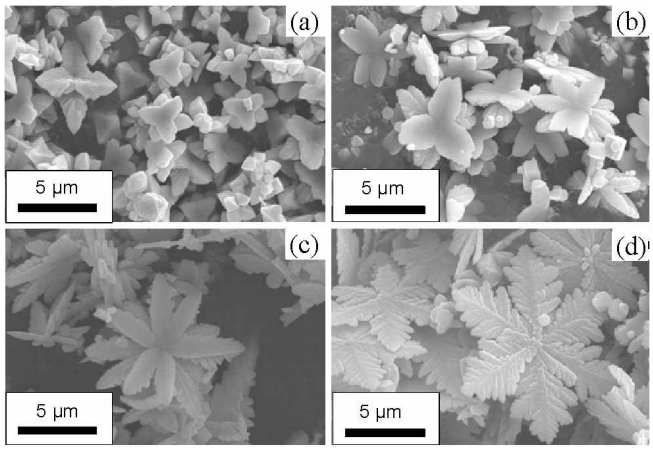

Figure 4. SEM images of α-Fe_2O_3 products obtained at [KCN] = 1.50 M using different concentrations of $FeCl_3$: (a) 0.001 M, (b) 0.005 M, (c) 0.01 M, and (d) 2.00 M.

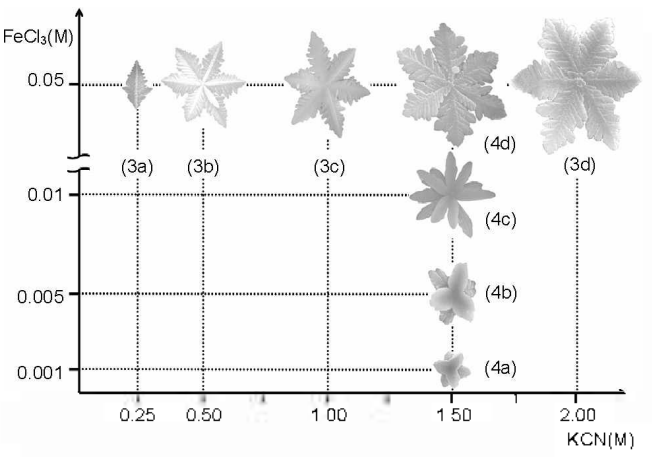

Figure 5. (a) Schematic illustration of the shape evolution of α-Fe_2O_3 crystals.

Figure 3 shows SEM images of the α-Fe_2O_3 crystals obtained by reacting aqueous solutions of different concentrations of KCN and 0.05 M $FeCl_3$. When the concentration of KCN is 0.25 M, pine tree-like α-Fe_2O_3 crystals of average length 2 μm were formed (Figure 3a). This pine tree morphology exhibits symmetrically disposed branches and side- branches about a single central axis. The crystals began to resemble snowflakes with a six-fold center of symmetry and an average arm length of 3.5 μm at 0.50 M KCN (Figure 3b). When the concentration of KCN is increased to 1.00 M, these crystals increased in size to an average arm length of 4 μm. As might be expected, the main arms of the crystals were at almost 60° to each other, and similarly, side-branches also formed an angle of 60° with the main crystal arms (Figure 3c). At 2.00 M KCN, the side-branches grew more so and became interconnected and adopted a snowflake-like appearance with an average arm length of 5.5 μm (Figure 3d). Therefore, as the concentration of KCN was increased from 0.05 M to 2.00 M, while keeping the concentration of $FeCl_3$ constant at 0.05 M, the morphology of the α-Fe_2O_3 changes from the pine tree-like crystals of 2 μm length to sharp snowflake-like crystals of 3.5 μm length, and finally to smooth snowflake-like crystals of 5.5 μm length.

To investigate the effect of concentration of $FeCl_3$, the α-Fe_2O_3 crystals were prepared by reacting aqueous solutions of different concentrations of $FeCl_3$ with fixed 1.50 M KCN as shown in Figure 4. When the concentration of $FeCl_3$ was 0.001 M, star-like α-Fe_2O_3 crystals were formed (Figure 4a). The three dimensional star-like α-Fe_2O_3 crystals have six arms with 1.5 μm lengths extending outside from a center. When the concentration of $FeCl_3$ was increased to 0.005 M, the product was a mixture of paired three-leaf crystals and paired six-leaf crystals (Figure 4b). The length of each leaf is about 2.5 μm. As we can see from Figure 4b that one side of the leaf is smooth, whereas the other is striped. These paired crystals have face-to-face crystal growth pattern. The stripped face tends to pair with another stripped face. Therefore, the paired three-leaf and six-leaf crystals have two-dimensional structures such as paired plates. When the concentration of $FeCl_3$ was further increased to 0.01 M, the paired six-leaf crystals were formed with each leaf of 4 μm length (Figure 4c). Finally, the snowflake-like crystals of 5.3 μm length without any paired three-leaf and six-leaf crystals were obtained at

0.05 M $FeCl_3$ (Figure 4d). Therefore, as the concentration of $FeCl_3$ was increased from 0.001 M to 0.05 M at fixed 1.50 M KCN, the morphology of the α-Fe_2O_3 changes from the small size of three dimensional star-like crystals to the middle size of two dimensional paired three-leaf and six-leaf shaped crystals, and finally to the large size of snowflake- like crystals. Fig. 5 shows schematically the shape evolution of α-Fe_2O_3 from the pine tree-like to the snowflake-like and from the star-like to the snowflake-like with increasing the concentrations of KCN and $FeCl_3$, respectively.

Since CN^- ion is a very strong ligand, it was expected to chelate Fe^{3+} to form $[Fe(CN)_6]^{3-}$. The formation constant of $[Fe(CN)_6]^{3-}$ at 25 °C is about $1 \times 10^{42.17}$. However, $[Fe(CN)_6]^{3-}$ dissociates slowly into Fe^{3+} ions under hydrothermal conditions, and these ions react with OH^- under basic conditions to form $Fe(OH)_3$, which on dehydration forms α-Fe_2O_3. The set of chemical reactions involved in the formation of α-Fe_2O_3 are as follows:

$$Fe^{3-}(aq) + 6\ CN^-(aq) \rightleftharpoons [Fe(CN)_6]^{3-}(aq) \quad (1)$$

$$[Fe(CN)_6]^{3-}(aq) \rightarrow Fe^{3-}(aq) + 6\ CN^-(aq) \quad (2)$$

$$Fe^{3-}(aq) + 3\ OH^-(aq) \rightarrow [Fe(OH)_3] \quad (3)$$

$$2\ [Fe(OH)_3] \rightarrow \alpha\text{-}Fe_2O_3 + 3\ H_2O \quad (4)$$

The concentrations of KCN and $FeCl_3$ play important roles in the formation of various morphologies such as a star, paired three-leaf, paired six-leaf, pine tree, and snowflake. The unique shaped crystals of α-Fe_2O_3 could form because of the slow release of Fe^{3-} ions due to the stability of the $[Fe(CN)_6]^{3-}$ complex, which allows sufficient time for self-assembly to produce the crystals having morphologies of star, paired three-leaf, paired six-leaf, pine tree, and snowflake.

As the concentration of $FeCl_3$ is increased, the morphology of the α-Fe_2O_3 crystals varies from star-like to snowflake-like via paired three-leaf and six-leaf shapes. In general, the shape of crystals can be explained in terms of the growth rates along <001> and <111>. For star-like crystals having six arms to form, the growth rate along <100> is almost equal to those along <010> and <001>. This means that the crystal growth along x, y and z axes are preferred for the star-like crystals. However, paired three-leaf, paired six-leaf, and snowflake-like shapes α-Fe_2O_3 crystals have two-dimensional structures. For these two dimensional shapes of α-Fe_2O_3 crystals to form, the growth rate along <001> is must be slower than those along <100> and <010>. The crystal growth along z axis is hindered at higher concentration of $FeCl_3$ to form two dimensional crystals. When the concentration of $FeCl_3$ was increased to 0.005 M form 0.001 M, the crystals tend to be grown along the plane compared to the axis. The star-like crystals changed to three-leaf shaped which have three leaves on the top plate and other three leaves on the bottom plate. As the crystals are grown further by increasing the concentration of $FeCl_3$, the paired six-leaf shaped crystals are formed by splitting three leaves to six leaves. Finally, the snowflake-like crystals are formed by taking apart the paring of the paired six-leaf shaped crystals. Therefore, $FeCl_3$ plays important role in change of crystal morphology from three dimensional star-like crystals to two dimensional snowflake-like crystals.

The evolution of α-Fe_2O_3 crystal morphologies with the concentration of KCN from pine tree to snowflake can be also explained by a simple crystal growth mechanism. As the concentration of KCN increases, crystal morphology changed from a pine tree-like to a snowflake-like morphology. On increasing the concentration of CN^- ions, the self-assembly reaction rate of α-Fe_2O_3 increases and progressive branching steps are initiated. The first crystal growth started at the main arm at an angle of 60° to form a pine tree-like shape, and when branching crystal growth was started at arms with a six-fold symmetry, the snowflake morphology was formed by secondary growth. Finally they form snowflakes with wide branches by the third phase of crystal growth. Furthermore, these morphologies have two-dimensional structures, and thus, crystal growth perpendicular to the crystal plane is appreciably slower than that in the crystal plane. Therefore, KCN does not affect the crystal growth along z axis but the crystal planes. The formation of two-dimensional hyperbranched structures appears to depend on reaction rate in the crystal plane. When the concentration of KCN was increased, the rate of formation of α-Fe_2O_3 also increased and higher-order hyperbranched crystals with wide branches were formed.

In conclusion, we have synthesized various shapes of α-Fe_2O_3 crystals by hydrothermal reaction between KCN and $FeCl_3$ in aqueous solution. The concentrations of KCN and $FeCl_3$ were found to substantially affect the shape of the hyperbranched crystal structures produced. The shape evolution of α-Fe_2O_3 from pine tree-like to snowflake-like and from star-like to snowflake-like can be explained by simple crystal growth mechanism.

Acknowledgments. This work was supported by the GRRC program of Gyeonggi province (66971).

References

1. Antonietti, M.; Ozin, G. A. *Chem. Eur. J.* **2004**, *10*, 28.
2. Mann, S. *Angew. Chem. Int. Ed.* **2000**, *2839*, 3392.
3. Song, H. C.; Park, S. H.; Huh, Y. D. *Bull. Kor. Chem. Soc.* **2007**, *28*, 477.
4. He, K.; Xu, C. Y.; Zhen, L.; Shao, W. Z. *Mater. Lett.* **2008**, *62*, 739.
5. Chen, X.; Wang, X.; Wang, Z.; Yang, X.; Qian, Y. *Cryst. Growth Des.* **2005**, *5*, 347.
6. Wu, Z.; Pan, C.; Yao, Z.; Zhao, Q.; Xie, Y. *Cryst. Growth Des.* **2006**, *6*, 1717.
7. Ma, Y.; Qi, L.; Ma, J.; Cheng, H. *Cryst. Growth Des.* **2004**, *4*, 351.
8. Bandara, J.; Mielczarski, J. A.; Kiwi, J. *Langmuir* **1999**, *15*, 7680.
9. Hayashi, K.; Iwasaki, K.; Morii, H.; Xia, B.; Okuyama, K. J. *Nanopart. Res.* **2001**, *3*, 149.
10. Jiang, J. Z.; Lin, R.; Lin, W.; Nielsen, K.; Morup, S.; DamJohansen, K.; Clasen, R. *J. Phys. D Appl. Phys.* **1997**, *30*, 1459.
11. NuLi, Y.; Zhang, P.; Guo, Z.; Munroe, P.; Liu, H. *Electrochim. Acta* **2008**, *53*, 4213.
12. Matijevic, E. *Chem. Mater.* **1993**, *5*, 412.
13. Pu, Z.; Cao, M.; Yang, J.; Huang, K.; Hu, C. *Nanotech.* **2006**, *17*, 799.
14. Han, Q.; Xu, Y. Y.; Fu, Y. Y.; Zhang, H.; Wang, R. M.; Wang, T. M.; Chen, Z. Y. *Chem. Phys. Lett.* **2006**, *431*, 100.
15. Mitra, S.; Das, S.; Mandal, K.; Chaudhuri, S. *Nanotech.* **2007**, *18*, 275608.
16. Jia, C.; Cheng, Y.; Bao, F.; Chen, D.; Wang, Y. *J. Cryst. Growth* **2006**, *294*, 353.
17. Cao, M.; Liu, T.; Gao, S.; Sun, G.; Wu, X.; Hu, C.; Wang, Z. L. *Angew. Chem. Int. Ed.* **2005**, *44*, 4197.
18. Zhang, X.; Sui, C.; Gong, J.; Su, Z.; Qu, L. *J. Phys. Chem. C* **2007**, *111*, 9049.
19. Hu, X.; Yu, J. C.; Gong, J. *J. Phys. Chem. C* **2007**, *111*, 11180.
20. de Faria, D. L. A.; Silva, S. V.; de Oliveira, M. T. *J. Raman Spectr.* **1997**, *28*, 873.